Publications

6-2011

Interactions and Focusing of Nonlinear Water Waves

Harihar Khanal
Embry-Riddle Aeronautical University

Stefan C. Mancas
Embry-Riddle Aeronautical University, mancass@erau.edu

Shahrdad Sajjadi
Embry-Riddle Aeronautical University, sajja8b5@erau.edu

Interactions and Focusing of Nonlinear Water Waves

Harihar Khanal[1], **Stefan C. Mancas**[1] **and Shahrdad G. Sajjadi**[2]

[1] *Department of Mathematics, Embry-Riddle Aeronautical University*

[2] *Center for Geophysics and Planetary Physics, Embry-Riddle Aeronautical University*

emails: `harihar.khanal@erau.edu`, `mancass@erau.edu`, `sajja8b5@erau.edu`

Abstract

A theoretical and computational study is undertaken for the modulational instabilities of a pair of nonlinearly interacting two-dimensional waves in deep water. It has been shown that the full dynamics of these interacting waves gives rise to localized large-amplitude wavepackets (wave focusing). The coupled cubic nonlinear Schrödinger (CNLS) equations are used to derive a nonlinear dispersion equation which give rise to new class of modulational instabilities and demonstrates the dependence of obliqueness of the interacting waves. The computations, due to nonlinear wave-wave interactions, waves that are separately modulationally stable can give rise to the formation of large-amplitude coherent wave packets with amplitudes several times that of the initial waves. In the case for the original Benjamin-Feir instability, in contrast, waves disintegrate into a wide spectrum.

Key words: water waves, coupled nonlinear Schrödinger, fast spectral algorithm

1 Introduction

Extremely large size waves (commonly known as freak, rogue or giant waves) are very common in the open sea or ocean and they pose major hazard to mariners. As early as 1976, Peregrine [11] suggested that in the region of oceans where there is a strong current present, freak waves can form when action is conncentrated by reflection into a caustic region. A variable current acts analogously to filamentation instability in laser-plasma interactions [8, 9]. Freak waves are very steep and is a nonlinear phenomena, hence they cannot be represented and described by a linear water wave theory. Zakharov [19] has noted that in the last stage of their evolution, their steepness becomes 'infinite', thereby forming a 'wall of water', such as that shown in Fig. 1. However, before such an instant in time, the

steepness is higher than one for the limiting Stokes wave and before breaking the wave crest reaches three to four (sometimes even more) times higher than the crests of neighboring waves. The freak wave is preceded by a deep trough appearing as a 'hole in the sea'. On the other hand, a characteristic life time of a freak wave is short, typically ten of wave periods or so. For example, if the wave period is fifteen seconds, then their life time is just few minutes. Freak wave appears almost instantly from a relatively calm sea. It is, therefore, easy to appriciate that such peculiar features of freak waves cannot be explained by means of a linear theory. Even the focusing of ocean waves is a preconditions for formation of such waves.

Figure 1: A photograph of a rouge wave, depicting the enormous height of the wave and its nonlinear character.

It is now quite common to associate appearance of freak waves with the modulation instability of Stokes waves. This instability (known as the Benjamin–Feir instability) was first discovered by Lighthill [7] and the detail of theory was developed independently by Benjamin and Feir [2] and by Zakharov [15]. Zakharov showed slowly modulated weakly nonlinear Stokes wave can be described by nonlinear Shrödinger equation (NLSE) and that this equation is integrable [16] and is just the first term in the hierarchy of envelope equations describing packets of surface gravity waves. The second term in this hierarchy was calculated by Dysthe [4].

Since the pioneer work of Smith [13], many researchers attempted (both theoretically or numerically) to explain the freak wave formation by NLSE. Among diversed results obtained by them there is one important common observation which has been made by

all, and that is, nonlinear development of modulational instability leads to concentration of wave energy in a small spatial region. This marks the possibility for formation of freak wave. Modulation instability leads to decomposition of initially homogeneous Stokes wave into a system of envelope solitons, or more strictkly quasi-solitons [17, 18].

This state can be called "solitonic turbulence", or "quasisolitonic turbulence".

In this paper, we consider the problem of a single solition in a homogeneous media, being subjected to modulational instability which eventually leads to formation of a system of soliton. We will show that the supercritical instability leads to maximum formation of soliton, concentrated in a small region. Moreover, in going through subcritical instability the solitons coagulate to early stages of supercritical instability.

Moreover, we investigate the full dynamics of nonlinearly interacting deep water waves subjected to modulational/filamentation instabilities. It is found that random perturbations can grow to form inherently nonlinear water wave structures, the so called freak waves, through the nonlinear interaction between two coupled water waves. The latter should be of interest for explaining recent observations in water wave dynamics.

2 Formulation of the problem

In a pioneering work, a theory for the modulational instability of a pair of two-dimensional nonlinearly coupled water waves in deep water, as well as the formation and dynamics of localized freak wave packets was presented [12]. Likewise we follow suite in derivation of CNLS equations. Thus, we use the CNLS equations derived by Onorato *et al.* [10], which are valid for a system of obliquely propagating waves. As in [10] we define the $x-$axis as the middle between the two directions of propagation. Thus we define wavenumbers as $\mathbf{k}_A = (k_{A,x}, k_{A,y}) \equiv (k, \ell)$ and $\mathbf{k}_B = (k_{B,x}, k_{B,y}) \equiv (k, -\ell)$ with the undestanding that both k and ℓ are positive. The frequencies ω_j of the two carrier waves ($j = A,\ B$) are then related to the wavevectors $\mathbf{k}_j$ by the dispersion relation for deep water waves [6] $\omega_j = \sqrt{g|\mathbf{k}_j|}$, where g is acceleration due to gravity. Accordingly, we may define $\omega_A = \omega_B = \sqrt{g\kappa}$, where κ is the wavenumber norm given by $\kappa \equiv \sqrt{k^2 + \ell^2}$.

Multiplying the system of two-dimensional CNLS equations given in [10] by i, we obtain

$$i\left(\frac{\partial A}{\partial t} + C_x \frac{\partial A}{\partial x} + C_y \frac{\partial A}{\partial y}\right) + \alpha \frac{\partial^2 A}{\partial x^2} + \beta \frac{\partial^2 A}{\partial y^2} + \gamma \frac{\partial^2 A}{\partial x \partial y} - \xi |A^2| A - 2\zeta |B|^2 A = 0\,, \quad (1)$$

and

$$i\left(\frac{\partial B}{\partial t} + C_x \frac{\partial B}{\partial x} - C_y \frac{\partial B}{\partial y}\right) + \alpha \frac{\partial^2 B}{\partial x^2} + \beta \frac{\partial^2 B}{\partial y^2} - \gamma \frac{\partial^2 B}{\partial x \partial y} - \xi |B^2| B - 2\zeta |A|^2 B = 0\,, \quad (2)$$

where A and B are the amplitudes of the slowly varying wave envelopes and the corresponding surface elevations are given by

$$\{\eta_A, \eta_B\} = \tfrac{1}{2}\{A(\mathbf{r}, t), B(\mathbf{r}, t)\} \exp(ikx + i\ell y - i\omega t) + \text{c.c.}$$

where c.c. denotes complex conjugate. The x and y components of the group velocity are given respectively by

$$C_x = \omega k/2\kappa^2 \quad \text{and} \quad C_y = \omega \ell/2\kappa^2$$

and the group velocity dispersion coefficients are

$$\alpha = \omega(2\ell^2 - k^2)/8\kappa^4, \quad \beta = \omega(2k^2 - \ell^2)/8\kappa^4 \quad \text{and} \quad \gamma = -3\omega\ell k/4\kappa^4.$$

Also, the nonlinearity coefficients (as in [10]) are given by $\xi = \omega\kappa^2/2$ and

$$\zeta = \omega(k^5 - k^3\ell^2 - 3k\ell^4 - 2k^4\kappa + 2k^2\ell^2\kappa + 2\ell^4\kappa)/2\kappa^2(k - 2\kappa).$$

It is now amply confirmed that the two-dimensional CNLS equations (1) and (2) has temporal solutions

$$A_{eq} = A_0 \exp[-i(\xi|A_0|^2 + 2\zeta|B_0|^2)t] \quad \text{and} \quad B_{eq} = B_0 \exp[-i(\xi|B_0|^2 + 2\zeta|A_0|^2)t],$$

and we may use these soloutions to derive the nonlinear dispersion relation. Thus, assuming a small linear harmonic perturbation with the wavevector $\mathbf{K} = (K, L)$ and the frequency Ω, around the equilibrium solution given by

$$A = [A_0 + \epsilon A_1 + O(\epsilon^2)] \exp[-i(\xi|A_0|^2 + 2\zeta|B_0|^2)t]$$

and

$$B = [B_0 + \epsilon B_1 + O(\epsilon^2)] \exp[-i(\xi|B_0|^2 + 2\zeta|A_0|^2)t]$$

where $\epsilon \ll 1$ is a real parameter. Substituting theses into equations (1) and (2), linearizing in ϵ, then separating the real and imaginary parts, combining the resulting equations, and Fourier transforming, we obtain the nonlinear dispersion relation

$$[(\Omega - C_x K - C_y L)^2 - \Omega_1^2][(\Omega - C_x K + C_y L)^2 - \Omega_2^2] = \Omega_c^4, \tag{3}$$

where

$$\Omega_1^2 = (\alpha K^2 + \beta L^2 - \gamma KL)(\alpha K^2 + \beta L^2 + \gamma KL + 2\xi|A_0|^2),$$

$$\Omega_2^2 = (\alpha K^2 + \beta L^2 + \gamma KL)(\alpha K^2 + \beta L^2 - \gamma KL + 2\xi|B_0|^2)$$

and

$$\Omega_c^4 = 16\zeta^2 |A_0|^2|B_0|^2 (\alpha K^2 + \beta L^2 - \gamma KL)(\alpha K^2 + \beta L^2 + \gamma KL).$$

For computational purposes, it is convenient to make variables dimensionless. Thus, defining the wave steepness by κA and κB, we make the wave amplitudes dimensionless according to $A_0 = A_0'/\kappa$ and $B_0 = B_0'/\kappa$. Similarly, the wavenumbers and frequencies are

made dimensionless in the following manner: $K' = K/\kappa$, $L' = L/\kappa$, $k' = k/\kappa$, $\ell' = \ell/\kappa$, and $\Omega' = \Omega/\omega$. The remaining coefficients are also made dimensionless, using the adoption

$$C'_x = \frac{C_x \kappa}{\omega} = \frac{k'}{2}, \qquad\qquad C'_y = \frac{C_y \kappa}{\omega} = \frac{\ell'}{2},$$

$$\alpha' = \frac{\alpha \kappa^2}{\omega} = \frac{2\ell'^2 - k'^2}{8}, \qquad \beta' = \frac{\beta \kappa^2}{\omega} = \frac{2k'^2 - \ell'^2}{8},$$

$$\gamma' = \frac{\gamma \kappa^2}{\omega} = -\frac{3\ell' k'}{4}, \qquad\qquad \xi' = \frac{\xi}{\omega k^2} = \frac{1}{2},$$

and

$$\zeta' = \frac{\zeta}{\omega k^2} = \frac{(k')^5 - (k')^3(\ell')^2 - 3k'(\ell')^4 - 2(k')^4 + 2(k')^2(\ell')^2 + 2(\ell')^4}{2(k' - 2)}.$$

Hence, Eqs. (1) and (2) will remain the same except all the variables are now replaced with their primed counterparts. Note that, $k' = \cos\theta$ and $\ell' = \sin\theta$, where θ is the angle between the wave directions.

We remark that, in what follows, we will drop the 'dash' notation for the sake of clarity.

3 Numerical Approach

The nonlinear strongly coupled system of equations (1) and (2) will be computed using a fast numerical algorithm based on the spectral method [3, 14] which is explained below.

3.1 Fourier Spectral Method

Let $S = A + B$ and $D = A - B$, and consider the following system of equations obtained from (1) and (2)

$$i\left(\frac{\partial S}{\partial t} + C_x \frac{\partial S}{\partial x} + C_y \frac{\partial D}{\partial y}\right) + \alpha \frac{\partial^2 S}{\partial x^2} + \beta \frac{\partial^2 S}{\partial y^2} + \gamma \frac{\partial^2 D}{\partial x \partial y} = g(S, D) \qquad (4)$$

$$i\left(\frac{\partial D}{\partial t} + C_x \frac{\partial D}{\partial x} + C_y \frac{\partial S}{\partial y}\right) + \alpha \frac{\partial^2 D}{\partial x^2} + \beta \frac{\partial^2 D}{\partial y^2} + \gamma \frac{\partial^2 S}{\partial x \partial y} = g(D, S) \qquad (5)$$

where

$$g(u, v) = \frac{1}{8}\left[(\xi + 2\eta)\left(|u + v|^2 + |u - v|^2\right)u + (\xi - 2\eta)\left(|u + v|^2 - |u - v|^2\right)v\right] \qquad (6)$$

First, we reduce the above system of PDEs (4)–(5) into a system of ODEs using Fourier transform. The Fourier transform of $u(x, y)$ is defined by

$$\mathcal{F}(u)(k_x, k_y) = \widehat{u}(k_x, k_y) = \frac{1}{2\pi} \int_{-\infty}^{\infty} \int_{-\infty}^{\infty} e^{-i(k_x x + k_y y)} u(x, y)\, dx\, dy, \qquad (7)$$

with the corresponding inverse

$$\mathcal{F}^{-1}(\widehat{u})(x,y) = u(x,y) = \frac{1}{2\pi} \int_{-\infty}^{\infty} \int_{-\infty}^{\infty} e^{i(k_x x + k_y y)} \widehat{u}(k_x, k_y) \, dk_x \, dk_y. \tag{8}$$

The function $\widehat{u}(k_x, k_y)$ can be interpreted as the amplitude density of u for wavenumbers k_x, k_y. Now, we take the Fourier transform of both (4) and (5) as

$$i\frac{d\widehat{S}_t}{dt} - \left(k_x C_x + \alpha k_x^2 + \beta k_y^2\right) \widehat{S} - k_y \left(C_y + \gamma k_x\right) \widehat{D} = \widehat{g(S,D)}, \tag{9}$$

$$i\frac{d\widehat{D}_t}{dt} - \left(k_x C_x + \alpha k_x^2 + \beta k_y^2\right) \widehat{D} - k_y \left(C_y + \gamma k_x\right) \widehat{S} = \widehat{g(D,S)}, \tag{10}$$

Let $k_x C_x + \alpha k_x^2 + \beta k_y^2 = p$ and $k_y \left(C_y + \gamma k_x\right) = r$. Then, the equations (9) and (10) can be written in the matrix form as

$$i\frac{d}{dt} \begin{pmatrix} \widehat{S} \\ \widehat{D} \end{pmatrix} = \begin{pmatrix} p & r \\ r & p \end{pmatrix} \begin{pmatrix} \widehat{S} \\ \widehat{D} \end{pmatrix} + \begin{pmatrix} \widehat{g(S,D)} \\ \widehat{g(D,S)} \end{pmatrix} \tag{11}$$

Computing the eigenvalues and eigenvectors the solution to (11) can be written as

$$\begin{pmatrix} \widehat{S} \\ \widehat{D} \end{pmatrix} = \frac{1}{2} \begin{pmatrix} e^{-i\lambda_1 t} + e^{-i\lambda_2 t} & -e^{-i\lambda_1 t} + e^{-i\lambda_2 t} \\ -e^{-i\lambda_1 t} + e^{-i\lambda_2 t} & e^{-i\lambda_1 t} + e^{-i\lambda_2 t} \end{pmatrix} \begin{pmatrix} \widehat{S}(0) \\ \widehat{D}(0) \end{pmatrix}$$

$$+ \frac{1}{2} \int_0^t \begin{pmatrix} e^{i\lambda_1 \tau} \left(\widehat{g(S,D)} - \widehat{g(D,S)} \right) \\ e^{i\lambda_2 \tau} \left(\widehat{g(S,D)} + \widehat{g(D,S)} \right) \end{pmatrix} d\tau \tag{12}$$

with $\lambda_1 = k_x C_x + \alpha k_x^2 + \beta k_y^2 - k_y \left(C_y + \gamma k_x\right)$ and $\lambda_2 = k_x C_x + \alpha k_x^2 + \beta k_y^2 + k_y \left(C_y + \gamma k_x\right)$.

3.2 Spatial discretization (Discrete Fourier Transform)

We discretize the spatial domain $\Omega = [-L/2, L/2] \times [-L/2, L/2]$ into $n \times n$ uniformly spaced grid points $X_{ij} = (x_i, y_j)$ with $\Delta x = \Delta y = L/n$, n even, and L the length of the rectangular mesh Ω. Given $u(X_{ij}) = U_{ij}$, $i, j = 1, 2, \cdots, n$, we define the 2D Discrete Fourier transform (2DFT) of u as

$$\widehat{u}_{k_x k_y} = \Delta x \Delta y \sum_{i=1}^{n} \sum_{j=1}^{n} e^{-i(k_x x_i + k_y y_j)} U_{ij}, \quad k_x, k_y = -\frac{n}{2} + 1, \cdots, \frac{n}{2} \tag{13}$$

and its inverse 2DFT as

$$U_{ij} = \frac{1}{(2\pi)^2} \sum_{k_x = -n/2+1}^{n/2} \sum_{k_y = -n/2+1}^{n/2} e^{i(k_x x_i + k_y y_j)} \widehat{u}_{k_x k_y}, \quad i, j = 1, 2, \cdots, n. \tag{14}$$

In equation (13) and (14) the wavenumbers k_x and k_y, and the spatial indexes i and j, take only integer values.

3.3 Temporal discretization

We solve the initial value problem of the ODE system (11) using the classical fourth order Runge-Kutta (RK4) method combined with the Super–Time–Stepping (STS) [1] and exact treatment for the linear part [3].

Given $t_{\max}$, we discretize the time domain $[0, t_{\max}]$ with equal time steps of size Δt with $t_n = n\Delta t$, $n = 0, 1, 2, \cdots$, and define $S^n = S(x, y; t_n)$ and $D^n = D(x, y; t_n)$. Initializing $\widehat{S}^n = \widehat{S}(t_n)$ and $\widehat{D}^n = \widehat{D}(t_n)$, we compute the Fourier transforms of the nonlinear terms $\mathcal{F}\left(g\left(\mathcal{F}^{-1}(\widehat{S}^n), \mathcal{F}^{-1}(\widehat{D}^n)\right)\right)$ and $\mathcal{F}\left(g\left(\mathcal{F}^{-1}(\widehat{D}^n), \mathcal{F}^{-1}(\widehat{S}^n)\right)\right)$, and advanced the ODE (11) in time with time step Δt using the explicit RK4 for the nonlinear part, together with an exact solution for the linear part as shown in (12). We exploit symmetry of the nonlinear function g in developing a numerical code to solve the system of ODEs (11). To overcome stability restriction on the stepsize Δt, we employ Super–Time–Stepping (STS) strategy [1].

The main idea behind the STS is to demand stability restriction only at the end of every N steps, consisting one super–step, instead of at every single step. The intermediate steps are chosen non–uniformly from a simple formula in terms of some modified Chebychev polynomials as

$$\tau_i = \frac{\Delta t}{(-1 + \nu)\cos\left(\frac{2i-1}{N}\frac{\pi}{2}\right) + 1 - \nu}, \quad i = 1, 2, \cdots N, \quad 0 < \nu < 1. \tag{15}$$

As $\nu \to 0$, the duration of the superstep $\Delta t_{\sup} = \sum_{i=1}^{N} \tau_i \to N^2 \Delta t$. Thus, N substeps of a super step cover a time interval N times bigger than N explicit steps when $\nu \to 0$. For each choice of N, the scheme is stable for large enough ν. The larger the damping factor ν, the shorter the $\Delta t_{\sup}$ becomes, improving the accuracy at the expense of more computations. The length of the superstep $\Delta t_{\sup}$, which is determined by the choice of N, ν and Δt, is only restricted by accuracy, just like in any unconditionally stable implicit methods.

The numerical code for the above procedure is implemented in Fortran 90 and executated on a linux cluster (of 128 nodes with dual Xeon 3.2GHz processors, 1024 KB cache 4GB with Myrinet) at Embry-Riddle Aeronautical University.

3.4 Simulation setup

The initial profiles for A and B were taken as the bell-shaped functions,

$$A(x, y; 0) = (A_0 + random(O(10^{-3}/\kappa))\, e^{-\sigma(x^2 + y^2)} \tag{16}$$

$$B(x, y; 0) = (B_0 + random(O(10^{-3}/\kappa))\, e^{-\sigma(x^2 + y^2)} \tag{17}$$

In the simulations reported here, we used the parameter values $\theta_0 = \pi/6$, $g = 9.81$, $w = 0.56$, $k = 0.33$, $A_0 = 0.1/\kappa$, $B_0 = A_0, 0$, $\sigma = 1, 0$, $L = 2$ and a grid of 256×256 nodes in the computational domain $[-1, 1] \times [-1, 1]$ with the time stepsize $\Delta t = 0.01$.

For each simulation we monitor the energies $Q_A(t)$ and $Q_B(t)$, calculated as

$$Q_A(t) = \int_{-\infty}^{\infty} \int_{-\infty}^{\infty} |A(x, y; t)|^2 \, dx \, dy = \sum_{i=1}^{n} \sum_{j=1}^{n} |A_{ij}|^2 \Delta x \Delta y \tag{18}$$

$$Q_B(t) = \int_{-\infty}^{\infty} \int_{-\infty}^{\infty} |B(x, y; t)|^2 \, dx \, dy = \sum_{i=1}^{n} \sum_{j=1}^{n} |B_{ij}|^2 \Delta x \Delta y \tag{19}$$

Observing a finite energy will reveal stability of a solution. As soon as the solution becomes unstable, the energy diverges. When the solution dissipates the energy approaches to zero.

4   Results

We commence this section by emphasizing that the results presented in this paper represents a very preliminary findings on dynamics of interacting nonlinear water waves. In due course, the full account of our findings will be reported elsewhere. The main emphasis here is the numerical methodologies for solution of equations (1) and (2).

The problem considered here comprises the dynamics of nonlinear interacting water wave packets through solving the coupled system of equations (1) and (2). The results of the simulation are displayed in Fig. 2 and Fig. 3. In this simulation, we have adopted the normalization $A' = A/\kappa$, $B' = B/\kappa$, $t' = \omega t$, $x' = \kappa x$, and $y' = \kappa y$ (the other scaled parameters are as those given above), for a single value of $\theta = \pi/6$. The results that are shown in Fig. 2 are all in dimensional units, where the two interacting waves initially have the amplitude $A = B = 0.1/\kappa + \text{ran}$, with ran representing a random low-amplitude noise, equal to $10^{-3}/\kappa$, in order to enhance instability. The results shown in Fig. 2 represent different time steps (starting on the left-hand panel and going downwards) for $t = 300/\omega$, $t = 600/\omega$, $t = 900/\omega$ then (right-hand panel) $t = 1200/\omega$, $t = 1500/\omega$; the last figure on the right-hand panel is at the same time as that above it but plotted from a different prospective reflecting the maximum growth rate in the y direction. For our simulations we have taken typical data from ocean waves [5]. Thus, choosing the frequency to be 0.09 Hz, we have $\omega = 0.56\,\text{s}^{-1}$, and $\kappa = \omega^2/g \approx 0.033\,\text{m}^{-1}$. The waves A and B in Fig. 2, then have the initial amplitudes $|A| = |B| = 0.1/\kappa \approx 3$ meters. From these figures, we see at $t = 1500/\omega$ (≈ 2680 seconds) that wave A focouses as a localized wave packets with a maximum amplitude of $\approx 0.35/\kappa \approx 10$ meters. We remark for considerable period after the initial step, waves A and B are qualitatively the same (with $|A| > |B|$) before the nonlinear wave-wave interactions set in which results to wave break-up.

We next consider the case of a single wave we have set B to zero, being the same as the standard Benjamin-Feir instability. In this case (see Fig. 3.), we do not see the formation of well-defined wave-packets, but the instability gave rise to a wide spectrum of waves in
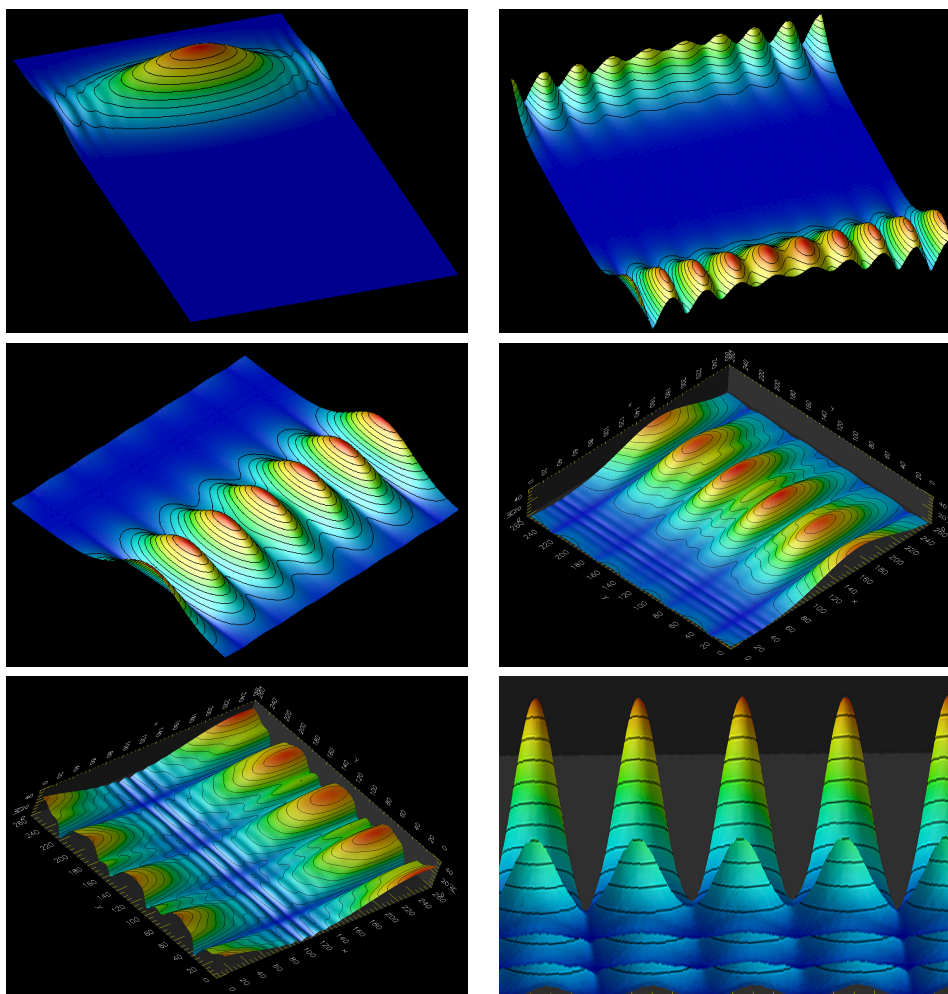
Figure 2: The interaction between two waves, with equal initial amplitudes $|A| = |B| = 0.1\,\kappa^{-1}$ which are propagating at an angle of $\theta = \pi/6$. A low-amplitude noise equal to $10^{-3}/\kappa$ is added to the initial amplitude in order to enhance the modulation instability.
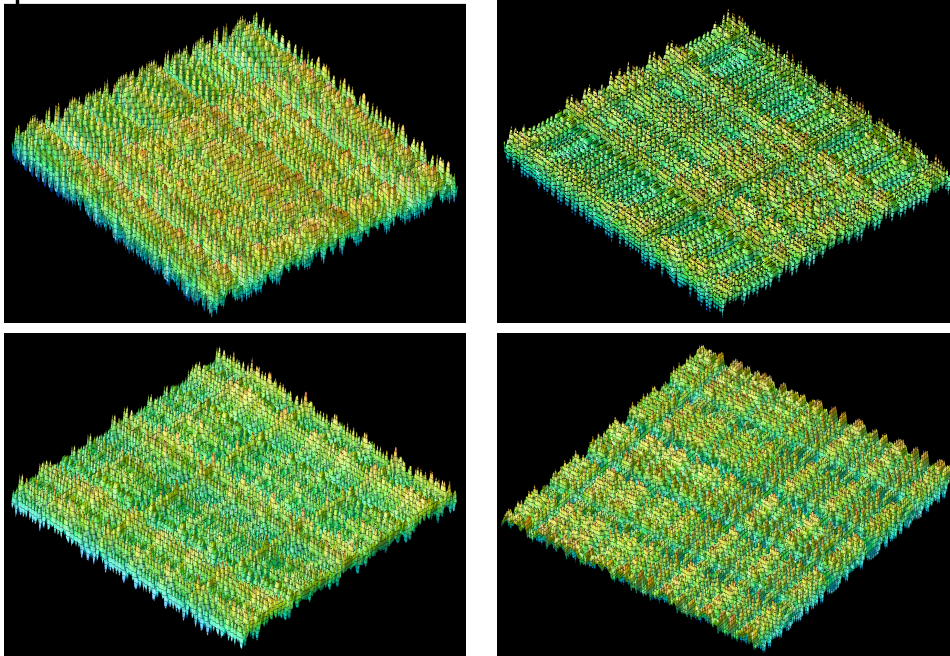
Figure 3: The amplitude $|A|$ (with $B = 0$ initially) for time $t = 300/\omega$, $t = 900/\omega$ (left-hand panel) and $t = 1200/\omega$, $t = 1500/\omega$ (right-hand panel).

different directions, in agreement with the standard linear analysis. This is in contrast with the new instability due to the coupling of the two waves, shown in Fig. 2., which has a well-defined maximum in the y direction, with the concentration of wave energy into localized wavepackets.

Hence, in summary, we have presented a theoretical and computational study of the modulational instabilities of a pair of nonlinearly interacting two-dimensional waves in deep water. we have demonstrated that the full dynamics of these interacting waves gives rise to localized large-amplitude wavepackets. Starting from the CNLS equations of [10] and following [12], we have derived a nonlinear dispersion equation which give rise to new class of modulational instabilities demonstrating the dependence of obliqueness of the interacting waves. Furthermore, the numerical analysis of the full dynamical system reveals that even waves that are separately modulationally stable can, when nonlinear interactions are taken into account, give rise to novel behavior such as the formation of large-amplitude coherent wave packets with amplitudes several times the initial waves. This behavior is quite different from that of a single wave (the case for the original Benjamin-Feir instability) which disintegrates into a wide spectrum of waves. These results are relevant to the nonlinear

HARIHAR KHANAL, STEFAN MANCAS, SHAHRDAD SAJJADI

instability arising from colliding water waves thereby producing large-amplitude oceanic freak waves.

Acknowledgements

References

[1] V. ALEXIADES, G. AMIEZ, AND P.A. GREMAUD, *Super-Time-Stepping acceleration of explicit schemes for parabolic problems*, Communications in Numerical Methods in Engineering, **12**, (1996), 31–42.

[2] T. B. BENJAMIN AND J. E. FEIR, *The desintegration of wave trains on deep water. Part 1. Theory*, J. Fluid Mech. **27** (1967) 417–430.

[3] G. BEYLKIN, J.M. KEISER, L. VOZOVOI, *A New Class of Time Discretization Schemes for the Solution of Nonlinear PDEs*, J. Comp. Physics. **147** (1998) 362–387.

[4] K. B. DYSTHE, *Note on a modification to the nonlinear Schrodinger equation for application to deep water waves*, Proc. Roy. Ser. A **369** (1979) 105–114.

[5] K. HASSELMANN, W. SELL, D. B. ROSS, P. MÜLLER, *A parametric wave prediction model*, J. Phys. Oceanogr. **6**, 200 (1976).

[6] V. I. KARPMAN, *Nonlinear Waves in Dispersive Media*, Pergamon Press, New York, 1975.

[7] M. J. LIGHTHILL, *Contribution to the theory of waves in nonlinear dispersive systems*, J. Inst. Math. Appl. **1** (1965) 269–306.

[8] D J NICHOLAS AND S G SAJJADI, *Numerical simulation of filamentation in laser-plasma interactions*, J. Phys. D: Appl. Phys. **19** (1986) 737–749.

[9] D. J. NICHOLAS AND S. G. SAJJADI, *The effect of light filamentation on uniformity of energy deposition in laser plasmas*, J. Plasma Physics **41** (1989) 209–218.

[10] M. ONORATO, A. R. OSBORNE, AND M. SERIO, *Modulational Instability in Crossing Sea States: A Possible Mechanism for the Formation of Freak Waves*, Phys. Rev. Lett. **96** (2006) 014503-6.

[11] H. PEREGRINE, *Interaction of water waves and currents*, Adv. Appl. Mech. **16** (1976), 9–117.

[12] P. K. SHUKLA, I. KOURAKIS, B. ELIASSON, M. MARKLUND, AND L. STENFLO, *Instability and Evolution of Nonlinearly Interacting Water Waves*, Phys. Rev. Lett. **97** (2006) 094501-4.

[13] R. SMITH, *Giant Waves*, Fluid Mech. **77** (1976), 417– 431.

[14] L. N. TREFETHEN, *Spectral Methods in Matlab*, Society for Industrial and Applied Mathematics (SIAM), Philadelphia, PA, 2000.

[15] V. E. ZAKHAROV, *Stability of periodic waves of finite amplitude on a surface of deep fluid*, J. Appl. Mech. Tech. Phys. **9** (1968) 190–194.

[16] V. E. ZAKHAROV, A. B. SHABAT, *Exact theory of two-dimensional self-focusing and one-dimensional self-modulation of waves in nonlinear media*, Soviet Physics JETP **34** (1972) 62–69.

[17] V. E. ZAKHAROV AND E. A. KUZNETSOV, *Optical solitons and quasisolitons*, JETP **86** (1998) 1035– 1046.

[18] V. E. ZAKHAROV, F. DIAS AND A. N. PUSHKAREV, *One-Dimensional Wave Turbulence*, Phys. Reports **398** (2004) 1–65.

[19] V.E. ZAKHAROV AND L.A. OSTROVSKY, *Modulation instability: The beginning*, Physica D **238** (2009) 540–548.